Analysis Of Novel PBI/ZrP Hybrid Membrane-based CuCl-HCl Electrolytic System On The Performance Of Hydrogen Production By FFD And RSM

Mohd Fadhzir Ahmad Kamaroddin[1,2,3*], Nordin Sabli[1,4*], Tuan Amran Tuan Abdullah[2,3], Luqman Chuah Abdullah[1], Shamsul Izhar[1], Nurul Sahida Hassan[2], and Aishah Abdul Jalil[2,3]

[1] Department of Chemical and Environmental Engineering, Faculty of Engineering, Universiti Putra Malaysia, 43400 Serdang, Selangor, Malaysia

[2] Centre of Hydrogen Energy, Institute of Future Energy, Universiti Teknologi Malaysia, 81310 Skudai, Johor, Malaysia

[3] Faculty of Chemical and Energy Engineering, Universiti Teknologi Malaysia, 81310 Skudai, Johor, Malaysia

[4] Institute of Nanoscience and Nanotechnology (IONS), Universiti Putra Malaysia, 43400, UPM Serdang, Selangor, Malaysia

[*] Corresponding author. E-mail: mohdfadhzir@utm.my, nordin$_sab@upm.edu.my$

Received: Apr. 18, 2025; Accepted: Jun. 22, 2025

Currently, the Copper Chloride (CuCl) hydrogen electrolytic process is integrated into the CuCl thermochemical cycle, operating at low temperatures and relying on expensive Nafion and Nafionbased membranes. This study demonstrates significant innovation by introducing a polybenzimidazole/ zirconium phosphate (PBI/ZrP) hybrid membrane, which exhibits a four-fold increase in proton conductivity compared to pristine polybezimidazole (PBI), addressing the limitations of conventional Nafion membranes in high-temperature hydrogen production. In this research, we investigate a high-temperature CuCl hydrogen electrolytic process that utilizes a hybrid membrane as an alternative to Nafion for hydrogen production. For the optimization study, a pre-synthesized PBI/ZrP hybrid membrane was used, where its proton conductivity shows a four-fold increase compared to pristine PBI. Response surface methodology (RSM) with a central composite design (CCD) was employed. The optimized parameters- 116°C temperature, 0.773 A cm^{-2} current density, and 0.075 M CuCl concentration - yielded an optimal hydrogen production rate of 0.7167 cm^3 min^{-1}. The actual hydrogen yield from these parameters reached 0.7709 cm^3 min^{-1}, with only a 7.56% discrepancy from the predicted value. In conclusion, this study showcases the efficacy of the high-temperature CuCl hydrogen electrolytic process using a PBI/ZrP hybrid membrane as a superior alternative to Nafion. This process not only maximizes hydrogen output but also optimizes operating parameters, thereby reducing associated hydrogen production costs.

Keywords: CuCl hydrogen electrolytic process; Hybrid membrane; Proton conductivity; Response surface methodology (RSM); Optimization

http://dx.doi.org/10.6180/jase.202605_29(5).0012

1. Introduction

Hydrogen production via thermochemical water splitting has gained considerable attention due to its efficiency and potential for large-scale hydrogen generation [1, 2]. Several thermochemical cycles have been investigated, including hybrid sulfur (HyS), copper chloride (CuCl), ceriumchlorine (Ce − Cl), vanadium-chlorine (V − Cl), hybrid chlorine, copper-sulfate (Cu − SO4), and ironchloride (Fe − Cl) cycles [3, 4]. Among these, the CuCl thermochemical cycle has shown particular promise due to its efficiency in electrolysis, making it a strong candidate for sustainable hydrogen production. The CuCl cycle operates by electrochemically converting CuCl and HCl into $CuCl_2$ and hydrogen, offering a closed-loop process with minimal emissions [5, 6].

A crucial component of CuCl electrolysis is the proton exchange membrane (PEM), which separates the electrolytes while allowing proton transport between electrodes [7–10]. Perfluorosulfonic acid (PFSA) membranes, such as Nafion, have been widely used due to their high conductivity at low temperatures ($\leq 90°C$) [11–13]. However, these membranes suffer from several limitations: (1) high cost, (2) reduced proton conductivity at high temperatures, (3) significant copper ion permeability, which shortens membrane lifespan in CuCl electrolysis, and (4) structural degradation under elevated temperatures [14–16].

To overcome these limitations, researchers have explored alternative membranes, including polybenzimidazole (PBI)-based and composite hybrid membranes [17–19]. PBI membranes, particularly when modified with inorganic fillers such as zirconium phosphate (ZrP), have shown enhanced thermal stability, reduced copper permeability, and improved mechanical durability, making them strong candidates for high-temperature electrolysis [20, 21]. Several studies have reported the application of PBI/ZrP hybrid membranes in fuel cells and electrochemical systems, demonstrating their ability to sustain high-temperature operation, chemical resistance, and enhanced proton conductivity [22]. However, their performance in CuCl electrolysis remains unexplored [23], presenting a gap in current research. Given the demand for membranes that can sustain high temperatures (100-130 °C) while ensuring efficient proton conductivity and chemical stability, this study investigates a PBI/ZrP hybrid membrane for CuCl electrolysis, addressing the challenges associated with Nafion-based systems [24]. This study aims to analyze the performance of the PBI/ZrP hybrid membrane for hydrogen production in a $CuCl - HCl$ electrolytic system. Specifically, the work focuses on evaluating the impact of temperature, current density, and CuCl concentration on hydrogen yield, comparing experimental results with predicted models using Full Factorial Design (FFD) and Response Surface Methodology (RSM) to optimize process parameters [25, 26], and demonstrating the feasibility of PBI/ZrP hybrid membranes as a costeffective and thermally stable alternative to Nafion for high-temperature CuCl electrolysis.

2. Materials and methods

2.1. Materials

The materials and reagents utilized in this study are crucial components that underpin the exploration of the PBI/ZrP hybrid membrane-based $CuCl - HCl$ electrolytic system. The choice of the proton-conductive polymer membrane, polybenzimidazole (PBI), is rooted in its exceptional thermal and chemical stability, making it an ideal facilitator of proton transport in electrochemical reactions. Further, the introduction of zirconium phosphate (ZrP) nanoparticles into the PBI matrix elevates proton conductivity and membrane stability, especially under demanding operating conditions.

The PBI/ZrP membrane used in this research was prepared based on the method described by Kamaroddin et al. [27] in their study titled "Phosphoric acid doped composite proton exchange membrane for hydrogen production in medium-temperature copper chloride electrolysis".

For the preparation, PBI membranes were dissolved in dimethylacetamide (DMAc) at 60 °C to form a 5 wt% PBI solution. Then, 10 wt% zirconium oxide (ZrO_2) was added to the solution. The mixture was stirred continuously for three hours and sonicated for an additional two hours to ensure even dispersion of ZrO_2. The resulting solution was spread onto a glass plate, dried under vacuum at 80 °C for 24 hours, and then carefully removed. Acid doping was conducted using phosphoric acid (PA) at a temperature range of 40-100 °C for 80 minutes to enhance proton conductivity.

The selection of the PBI/ZrP membrane in this study is based on its previously demonstrated thermal stability, mechanical strength, and enhanced proton conductivity, as reported in our earlier work [27]. These properties make it a promising candidate for high-temperature electrolysis applications, especially as an alternative to conventional Nafion membranes.

2.2. Methods

2.2.1. *Electrolytic Cell Setup*

The membrane electrode assembly (MEA) used in this study consisted of carbon cloth electrodes loaded with 0.5 $mgcm^{-2}Pt/C$ (60 % platinum on Vulcan) on both the anode and cathode sides, as reported in our previous work [27]. The MEA was assembled using Teflon gaskets, graphite flow plates with serpentine channels, and titanium end blocks to ensure proper compression and uniform gas flow within the electrolytic cell.

The electrolytic cell, a cornerstone of the hydrogen production process, was meticulously assembled to facilitate the electrochemical reactions within the PBI/ZrP hybrid membrane-based $CuCl - HCl$ electrolytic system. By applying an external voltage across the circuit via the solid proton exchange membrane (PEM), this setup enabled controlled cathode (hydrogen evolution reaction) and anode (oxygen evolution reaction) reactions within the electrolyte.

2.2.2. Operational Parameters

To systematically assess the system's performance, this study meticulously examines the influence of several operational parameters. Notably, the experimental exploration encompasses operating temperatures, CuCl concentrations, current densities, and CuCl flow rates. The selected ranges for each parameter were meticulously chosen based on insights gleaned from established studies utilizing Nafion membrane-based CuCl electrolytic systems. The important parameters from the established nafion membrane-based CuCl electrolytic systems are concluded in Table 1. This adaptation reflects the pioneering nature of our investigation in the context of PBI-based hybrid membranes.

Table 1. The parameters from the established Nafion membrane-based CuCl electrolytic systems

Parameters	Range
Temperature	100 to 130°C
CuCl concentration	0.01 to 0.2 M
Current densities	0.1 to 1.0 A cm^{-2}
CuCl flow rates	3 to 9 cm^3 min^{-1}

2.2.3. Full Factorial Design (FFD) and Response Surface Methodology (RSM)

To systematically unveil the intricate interactions between operational parameters and their impact on hydrogen production performance, this research harnessed two robust methodologies: Full Factorial Design (FFD) and Response Surface Methodology (RSM) by using Minitab 18 software. The FFD enabled a comprehensive exploration of variable effects, both individually and in combination, while the RSM facilitated the prediction of optimal parameter configurations to achieve desired hydrogen production outcomes.

2.2.4. Analysis and Measurements

A range of analytical techniques was carefully utilized to measure and interpret the key performance metrics, including hydrogen production rates and system efficiency. Gas Chromatography (GC) was applied to analyze the composition of the generated gases and confirm hydrogen purity. Electrochemical Impedance Spectroscopy (EIS) was used to determine proton conductivity values, showing that the PBI/ ZrP membrane exhibited significant improvement compared to pristine PBI. Thermogravimetric Analysis (TGA) and tensile strength testing were conducted to evaluate the thermal and mechanical stability of the hybrid membrane under hightemperature operating conditions. Table 2 gives a series of analysis conducted for measuring the performance of CuCl − HCl electrolytic system.

2.2.5. Data Collection and Processing

The acquired experimental data underwent rigorous collection and meticulous processing to unveil meaningful insights. By leveraging advanced statistical analysis and modeling techniques, the research sought to illuminate correlations between operational parameters and hydrogen production performance. This analytical effort aimed to understand the complex relationships within the PBI/ZrP hybrid membrane-based CuCl − HCl electrolytic system.

3. Results and discussion

3.1. Membrane Characterization

The PBI/ZrP membrane employed in this study was comprehensively characterized and benchmarked against Nafion 117 and pristine PBI membranes, with details previously published by Kamaroddin et al. [27]. Thermogravimetric analysis (TGA) showed that the PBI/ZrP membrane exhibited excellent thermal stability, maintaining its structural integrity up to ∼ 600°C, in contrast to Nafion 117, which degraded significantly above 350 °C.

Proton conductivity was evaluated using electrochemical impedance spectroscopy (EIS), revealing that PA doping and ZrP incorporation enhanced conductivity by up to four times compared to pristine PBI, with a maximum value of 104.7 mS · cm^{-1} at 40 °C. Although this conductivity was slightly lower than Nafion 117 at elevated temperatures (e.g., 5.67 mS · cm^{-1} vs. 10.06 mS · cm^{-1} at 90 °C), the PBI/ZrP membrane demonstrated superior thermal and mechanical robustness, which is crucial for medium-temperature CuCl electrolysis.

Moreover, the PBI/ZrP membrane exhibited significantly reduced copper ion permeability (7.87×10^{-7} cm^2/s) compared to Nafion 117 $\left(1.7 \times 10^{-6}\ cm^2/s\right)$, further supporting its long-term durability and suitability for electrolysis applications.

These characterization results confirm that the membrane properties have been thoroughly analyzed, and its advantages over conventional Nafion membranes have been clearly demonstrated in terms of thermal stability, proton conductivity, and copper resistance.

3.2. Thermogravimetric Analysis (TGA)

TGA was conducted to evaluate the thermal stability of the PBI/ZrP hybrid membrane compared to Nafion. The results showed that Nafion 117 degraded rapidly at around 350 °C, while the PBI/ZrP hybrid membrane exhibited minimal weight loss up to 500 °C and remained stable up to 600-650 °C. This demonstrates the superior thermal resistance of the hybrid membrane, attributed to the

Table 2. The analysis conducted by using a specified equipment and the parameters

Analysis	Equipment	Parameters
Proton conductivity	Electrochemical Impedance Spectroscopy (EIS) by using Metrohm PGSTAT302N Potentiostat	Scm^{-1}
Thermogravimetric analysis	Shimadzu Thermogravimetric Analyzer	TGA (wt%), Temperature (°C)
Gas Chromatography analysis	Agilent 6890N Gas Chromatography – Thermal Conductivity Detector (TCD)	wt%
Tensile Strength	a 2.5 kN Lloyd LRX universal testing machine	MPa

strong molecular interaction between the PBI backbone, ZrO_2 filler, and phosphoric acid doping, making it more suitable for high-temperature electrolysis applications.

3.3. Phosphoric Acid (PA) Doping and Proton Conductivity:

Phosphoric acid (PA) doping significantly enhanced the proton conductivity of the PBI-based membranes. Among the tested membranes, the PA-doped PBI at 40 °C demonstrated the highest proton conductivity at 104.7 $mS \cdot cm^{-1}$, which was approximately four times greater than that of pristine PBI membranes. This increase was attributed to the effective incorporation of PA molecules into the membrane structure, which facilitated proton transport via both vehicular and Grotthuss mechanisms. However, further increasing the doping temperature beyond 40 °C led to membrane swelling and reduced mechanical strength, resulting in decreased conductivity. The hybrid PBI/ ZrP membrane achieved conductivity values comparable to the best-performing PAdoped PBI membranes, with improved thermal and mechanical stability. Electrochemical impedance spectroscopy (EIS) revealed that the membrane resistance was significantly reduced from 280Ω (pristine PBI) to 175Ω(PBI/ZrP), indicating a conductivity improvement of over 60% compared to pristine PBI and 43 % over PA-doped PBI.

3.4. Proton Conductivity Analysis

The PA-doped PBI/ZrP membrane achieved a proton conductivity of 104.7 mS/cm, measured at 40 °C, which represented a four-fold improvement over pristine PBI. This significant enhancement is attributed to the effective incorporation of phosphoric acid and the stabilizing effect of zirconium phosphate within the membrane matrix. Furthermore, temperature-dependent conductivity measurements showed a steady increase in conductivity with temperature, reaching 5.671 mS/cm at 90 °C, compared to 10.057 mS/cm for Nafion 117 at the same temperature. Although Nafion exhibited slightly higher conductivity at elevated temperature, the PBI/ZrP membrane demonstrated superior thermal and mechanical stability under high-temperature operating conditions, making it a more robust choice for CuCl electrolysis applications.

Additionally, copper ion permeability tests revealed that the PBI/ZrP membrane significantly reduced Cu^{2+} diffusion, achieving a value of 7.87×10^{-7} cm^2/s. This reduced permeability helps to minimize membrane degradation and cross-contamination during long-term electrolysis operation, further supporting the membrane's potential to replace Nafion in harsh operating environments.

3.4.1. *Performance of the PBI/ZrP Hybrid Membrane on a CuCl Hydrogen Electrolytic Hydrogen System*

Two sets of experiments were performed using a two-level RBD with four operating parameters (temperature, CuCl concentration, current density and CuCl flowrate) to determine the influence of these parameters on the hydrogen yield using a PBI/ZrP hybrid membrane. The sequence of the experiments was randomized by the design of experiments (DOE) in the Minitab version 18. The operating temperatures, CuCl concentrations, current densities and CuCl flowrates were ranging from 100 to 130 °C, 0.01 to 0.2M, 0.1 to 1.0 A cm^{-2} and 3 to 9 cm^3 min^{-1}, respectively. The selected range for each parameter was adapted from the established studies using the Nafion membrane based CuCl electrolytic system since there was a very limited study on the PBI based hybrid membrane. The hydrogen yield was measured using a water displacement method as the gas mass flowmeter was not suitable due to intermittent hydrogen production. The collected volume of the hydrogen is then divided by the time taken to displace a certain amount of water to get a hydrogen yield flowrate.

The analysis of variance was used to statistically proven the significance of the effects of the operating parameters towards hydrogen production. By referring to the Table 3, p-value of 0.05 for 95 % confidence level, the operating parameters that showed the p-value smaller than 0.05 were the applied current density and temperature with a p-value

Table 3. Analysis of variance table for the CuCl electrolytic system

Source	DF	Adj SS	Adj MS	F-Value	P-Value
Model	5	74.62	14.92	7.76	0.00
Blocks	1	12.91	12.91	6.71	0.02
Linear	4	61.72	15.43	8.03	0.00
Temperature (°C)	1	11.37	11.37	5.92	0.03
CuCl Concentration (M)	1	5.63	5.63	2.93	0.10
Current Density (A/cm^2)	1	44.21	44.21	23.00	0.00
Electrolyte Flowrate (cm^3/min)	1	0.51	0.51	0.26	0.61
Error	18	34.60	1.92		
Lack-of-Fit	2	2.34	1.17	0.58	0.57
Pure Error	16	32.27	2.02		
Total	23	109.22			

of 0.000 and 0.026 , respectively. However, both CuCl concentration and electrolyte were not significant (p-value > 0.05) with p value of 0.104 and 0.613 , respectively. The operating temperature and current density were statistically significant based on the p-value < 0.05 in the ANOVA table.

The four operating parameters were studied (Fig. 1): operating temperature, CuCl concentration, current density, and CuCl flowrate. Three parameters showed a positive increment except for the CuCl flowrate. The most significant upwards trend for the hydrogen production was the current density (0.01 to 1.0 A cm^{-2}) followed by the operating temperature (100 to 130 °C) and CuCl concentration (0.01 to 0.2 M). Higher current density and temperature enhanced the kinetic activity and thus elevated the proton transfer from anode to cathode, translating to the intensification of hydrogen evolution reaction (HER) [28, 29]. However, as the CuCl flow rate increases, the retention time of the electrolyte within the electrolytic cell decreases, which limits proton transfer and reduces hydrogen yield. This aligns with the findings of Toghyani et al. [30], who reported that higher flow rates disrupt proton transfer efficiency and lower hydrogen production in similar electrolytic systems. Beyond a certain threshold, increasing the flow rate further compromises the interaction between the electrolyte and the membrane, leading to diminished performance.

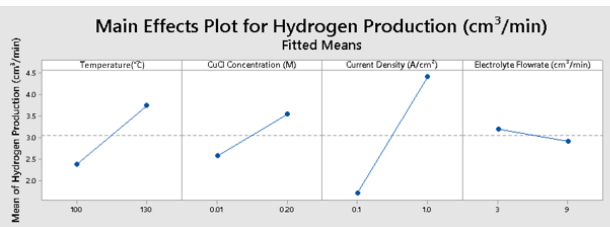

Fig. 1. The main effects plot for Hydrogen Production in CuCl electrolytic

This behavior is consistent with observations from studies on Nafion-based systems, where high flow rates and temperatures significantly reduce hydrogen yield due to the membranes' thermal instability and hydration dependency. In contrast, the PBI/ZrP hybrid membrane demonstrates improved thermal stability and conductivity, allowing it to maintain better hydrogen production performance under similar conditions. This highlights the advantages of using hybrid membranes in high-performance applications.

Additionally, excessively high current densities can generate excess heat within the system, disrupting electrochemical equilibrium and causing inefficiencies in the hydrogen evolution reaction (HER). Similarly, elevated CuCl concentrations may saturate the electrolyte, creating diffusion limitations and reducing proton availability for HER. These deviations from expected trends emphasize the necessity of a balanced optimization strategy. Excessively high parameter values can lead to secondary effects, such as electrolyte saturation and localized heating, which ultimately diminish the potential benefits of hydrogen production.

3.5. Optimization of CuCl Electrolytic System for Hydrogen production

3.6. Significant Parameters for Optimization of CuCl Electrolytic System

The normal plot of the standardized effects for the CuCl electrolytic system is illustrated in Fig. 2. Factor A and factor C represented the operating temperature and the applied current density, respectively. The current density had the standardized effect between 4.5 to 5, which responded to the increment above 80% for hydrogen production. Meanwhile, the increase in operating temperature reflected the rise of the hydrogen production of up to 60% with a 2.5 standardized effect. The normal probability plot shows whether the residuals follow a straight line to the normal probability distribution. It is used to evaluate the magnitude and statistical significance of linear, square and interaction effects. The fitted line represents where the points should fall if the effects were zero. Operating temperature (A) and applied current density (C) have significant influences that positively affect the right side of the graph, unlike CuCl concentration and electrolyte flowrate, which were insignificant.

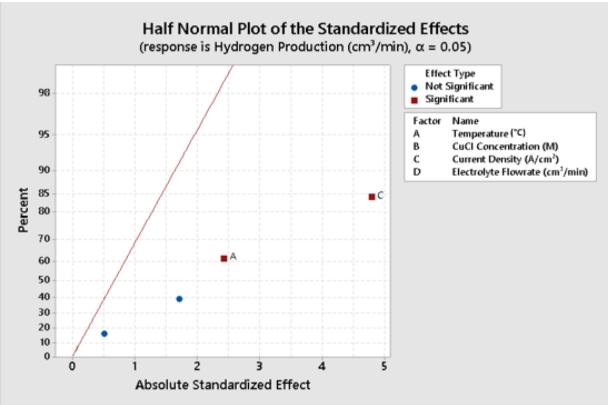

Fig. 2. The half normal plot of the standardized effects of the standardized effects of operating parameters on the CuCl electrolytic system

The interaction plots for the hydrogen production in the CuCl electrolytic system is illustrated in Fig. 3. Overall, the graph shows an incremental increase in hydrogen production for all the interactions when the operating parameters' range was enlarged from 100 to 130 °C for operating temperature, 0.01 to 0.2 M for CuCl concentration and 0.1 to 1.0 A cm^{-2} for applied current density. Four strong interaction plots were observed via the non-parallel lines: temperature versus CuCl concentration, temperature versus CuCl electrolyte, CuCl concentration versus CuCl electrolyte and current density versus CuCl electrolyte. These strong interactions plots show the significant influence of two parameters towards the hydrogen production. This strong interaction effect is essential in designing practical hydrogen production systems as it emphasizes the mutual dependence between operational variables.

From the interaction plots, we can conclude that a higher value of operating parameters does not necessarily produce a higher amount of hydrogen yield. Therefore, the interaction plots are useful to gauge the optimum operating parameters to get the highest hydrogen yield.

The findings of this study have significant implications for practical hydrogen production. The PBI/ZrP membrane not only achieves higher yields at elevated temperatures but also shows greater tolerance to variations in operating

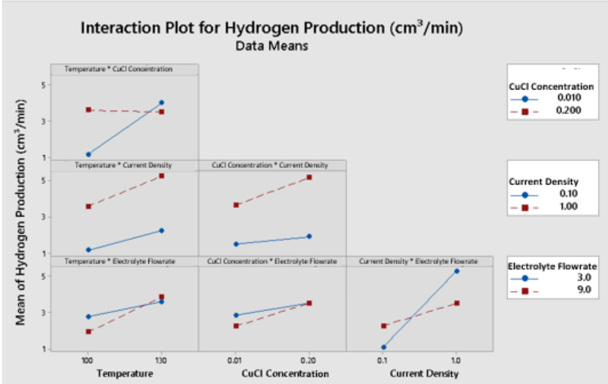

Fig. 3. The interaction plot for Hydrogen Production in CuCl electrolytic system; CuCl concentration (M), current density (A cm^{-2}) and Electrolyte flowrate (cm^3 min−1).

conditions, making it a strong candidate for large-scale applications. This is in contrast to conventional Nafion-based systems, which demand stricter control over operational parameters.

The main effects plot for hydrogen production (Fig. 4) displays that temperature at 130 °C was linked with the highest hydrogen production yield. Cross-checked with the two-way ANOVA results showed that the temperature was statistically significant with a p-value of 0.04 (less than 0.05). Applied current density at 0.55 A cm^{-2} was associated with the highest hydrogen production. However, the two-way ANOVA results showed that this main effect was not statistically significant (p-value $= 0.613$) that may occur by random chance. CuCl concentration at 0.105 M was associated with the highest hydrogen production. Nonetheless, its two-way ANOVA results also proven that this main effect was not statistically significant (p-value $= 0.993$). The two-way ANOVA results showed that the interaction between temperature, current density and CuCl concentration was not significant. Therefore, we cannot interpret the main effects without the interaction effect into consideration.

3.6.1. *Analysis of Variance for Optimization of CuCl Electrolytic System*

The analysis of variance (ANOVA) of the response surface methodology (RSM) by central composite design (CCD) was employed to determine statistically significant terms and estimate the regression coefficient of the model. The ANOVA was carried out with the Minitab 18 software programme with a p-value of 0.05. The percentage variability of the optimization parameter was also calculated using the R-squared statistic. Finally, the model's adequacy was assessed using the normal probability plot of the residuals and the plots of the residuals vs the anticipated responses.

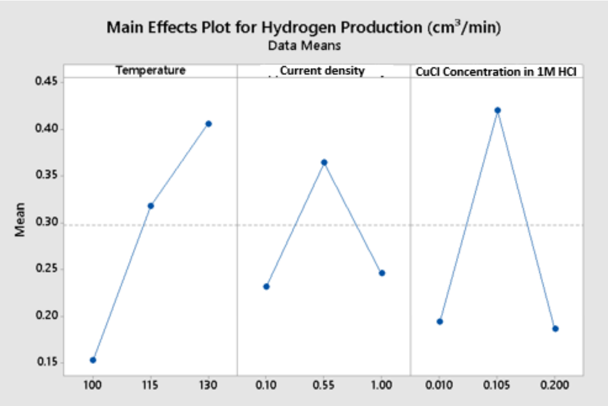

Fig. 4. The main effects plot for Hydrogen Production in CuCl electrolytic system

Surface response plots were used to demonstrate how a response variable is related to two variables using a model equation.

The p-values for all significant parameters were temperature with a p-value at 0.04 for linear, squared concentration*concentration with a p-value at 0.003. None of the 2-way interaction parameters was significant.

There were three significant parameters involved, which are temperature (°C), current density (A cm^{-2}) and CuCl concentration (M) at a 95% confidence level. The regression coefficients of process parameters for the CuCl electrolytic system are shown in Table 4. Factors of contribution and interaction are tabulated with detailed values to deduce the best fitting model equation. The predicted model (Eq. (1)) and simplified version (Eq. (2)) were deduced from the regression coefficients table.

The ANOVA of the CuCl electrolytic system is shown in Table 5 with p-value of less than 0.05 indicated that the factor has more than 95% confidence level. From the below-coded coefficients, the only temperature has a significant factor with p-value of 0.001. Meanwhile, the squared term coefficient for current density and CuCl concentration was significant with a p-value of 0.006 and 0.00, respectively. Therefore, it can be concluded that the relationship between the squared current density and squared CuCl concentration and the hydrogen production follows a curved line. There was no significant coefficient for interactions as all the p-value were above 0.05.

The regression equation in an uncoded unit can be represented by the following Eqs. (1) and (2).

$$
\begin{aligned}
&\text{Hydrogen Production}(\text{cm}^3\text{min}^{-1}) = \\
&\quad -5.08 + 0.0783\ \text{Temperature}\ (^\circ\text{C}) \\
&\quad + 0.514\ \text{Current Density}\ \left(\text{Acm}^{-2}\right) \\
&\quad + 9.43\ \text{Concentration CuCl(M)} \\
&\quad - 0.000297\ \text{Temperature}\ (^\circ\text{C}) * \text{Temperature}\ (^\circ\text{C}) \\
&\quad - 0.730\ \text{Current Density}\ \left(\text{Acm}^{-2}\right) * \text{Current Density}\ \left(\text{Acm}^{-2}\right) \\
&\quad - 27.21\ \text{Concentration CuCl(M)}^* \text{ Concentration CuCl(M)} \\
&\quad + 0.00299\ \text{Temperature}\ (^\circ\text{C}) * \text{Current Density}\ \left(\text{Acm}^{-2}\right) \\
&\quad - 0.0309\ \text{Temperature}\ (^\circ\text{C}) * \text{ConcentrationCuCl(M)} \\
&\quad - 0.38\ \text{Current Density}\ \left(\text{Acm}^{-2}\right)\ \text{ConcentrationCuCl(M)}
\end{aligned}
\tag{1}
$$

$$
\begin{aligned}
&\text{Hydrogen Production}\ \left(\text{cm}^3\ \text{min}^{-1}\right)\ \text{(simplified)} \\
&\quad = -5.08 + 0.0783\ A + 0.514\ B + 9.43C - 0.000297\ A^2 \\
&\qquad - 0.730\ B^2 - 27.21C^2 + 0.00299\ A^*\ B - 0.0309\ A^*C \\
&\qquad - 0.38\ B^*C
\end{aligned}
\tag{2}
$$

where A is the temperature (°C), B is current density $\left(\text{Acm}^{-2}\right)$, C is the CuCl concentration (M), and the dependent variable is the hydrogen production $\left(\text{cm}^3\ \text{min}^{-1}\right)$

3.6.2. *Optimization of CuCl Electrolytic Parameters*

The optimization of the CuCl electrolytic experiment using an RSM by CCD was trying to find the best settings of the parameters to get the optimum amount of hydrogen production. Prior to that, interaction plots for hydrogen production were tabulated to get the interaction between temperature, current density and CuCl concentration in Fig. 5.

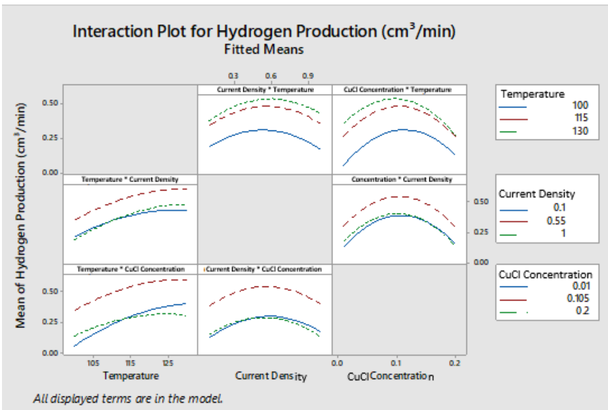

Fig. 5. Interaction plot for hydrogen production with CuCl electrolytic system parameters (temperature, current density and CuCl concentration)

Table 4. The regression coefficients of process parameters for the CuCl electrolytic system

Term	Coef	SE Coef	T-Value	P-Value	VIF
Constant	0.5426	0.0534	10.16	0	1
Temperature (°C)	0.1266	0.0327	3.87	0.001	1
Current Density (A/cm^2)	0.0069	0.0327	0.21	0.834	1
Concentration CuCl(M)	-0.0038	0.0327	-0.12	0.908	1
Temperature (°C)* Temperature (°C)	-0.0667	0.0481	-1.39	0.181	1.01
Current Density (A /cm^2)* Current Density (A/cm^2)	-0.1478	0.0481	-3.07	0.006	1.01
Concentration CuCl (M)*Concentration CuCl(M)	-0.2455	0.0481	-5.1	0	1.01
Temperature (°C) *Current Density (A/cm^2)	0.0202	0.0462	0.44	0.668	1
Temperature (°C)* Concentration CuCl(M)	-0.044	0.0462	-0.95	0.353	1
Current Density (A/cm^2)*Concentration CuCl(M)	-0.0161	0.0462	-0.35	0.732	1

Table 5. The Analysis of Variance (ANOVA) for the RSM CCD of the CuCl electrolytic system

Source	DF	Adj SS	Adj MS	F-Value	P-Value
Model	9	0.858	0.095	5.570	0.001
Linear	3	0.257	0.086	5.010	0.009
Temperature (°C)	1	0.256	0.256	14.980	0.001
Current Density (A/cm^2)	1	0.001	0.001	0.050	0.834
Concentration CuCl(M)	1	0.000	0.000	0.010	0.908
Square	3	0.580	0.193	11.300	0.000
Temperature (°C)* Temperature (°C)	1	0.033	0.033	1.920	0.181
Current Density (A/cm^2)* Current Density (A/cm^2)	1	0.161	0.161	9.430	0.006
Concentration CuCl(M)* Concentration CuCl(M)	1	0.445	0.445	26.020	0.000
2-Way Interaction	3	0.021	0.007	0.410	0.751
Temperature (°C)*Current Density (A/cm^2)	1	0.003	0.003	0.190	0.668
Temperature (°C)* Concentration CuCl(M)	1	0.016	0.016	0.910	0.353
Current Density (A/cm^2) * Concentration CuCl(M)	1	0.002	0.002	0.120	0.732
Error	20	0.342	0.017		
Lack-of-Fit	3	0.008	0.003	0.130	0.943
Pure Error	17	0.335	0.020		
Total	29	1.200			

From Fig. 5, it was observed that there were five interaction plots except for no interaction for current density vs temperature and CuCl concentration vs temperature. For temperature-based interaction plots, the interaction temperature occurred around 110 to 115°C while the CuCl concentration was at 0.01 and 0.2 M, and the current density was about 0.1 to 1 A cm^{-2}. The highest hydrogen production was achieved at 115°C.

For current density-based interaction plots, only CuCl concentration demonstrated the interaction with the current density at 0.45 A cm^{-2} while the CuCl concentration was at 0.01 and 0.2 M. Furthermore, for CuCl concentration-based interaction plots, only current density showed the interaction with the CuCl concentration at 0.15 M while the current densities were at 0.1 and 1 A cm^{-2}. Although the interaction plots gave some ideas about how the manipulation of the parameters influenced the hydrogen production, however, the interaction plots did not give the optimum value for the parameters to get the optimum hydrogen production. Therefore, the optimization process must be carried out.

The main effects plot for hydrogen production is shown in Figure 6. It shows the influence of temperature, current density and CuCl concentration on hydrogen production. From Fig. 6, the hydrogen production reached its maximum output when the temperature reached 125°C and above, the current density at 0.5 A cm^{-2} and the CuCl concentration was at 0.1 M. However, the figures in ere the individual influence of the parameters towards the hydrogen production. Hence, the optimization with Minitab 18 determined the best value of the parameters that gave the optimum hydrogen production.

Although the interaction plots describe a significant interaction among the parameters towards the hydrogen production, the value of the parameter given was not optimized to cater to all parameters to produce the optimum yield. Therefore, Table 6 displays the predicted response optimization for hydrogen production using Minitab 18

Table 6. Predicted response optimization for hydrogen production using Minitab 18

Response Optimization: Hydrogen Production (cm^3/min)

Optimization Plot

Prediction for Hydrogen Production (cm^3/min), StdOrder
Multiple Response Prediction

Variable	Setting
Temperature (°C)	116.67
Current Density (A/cm^2)	0.7727
Concentration CuCl(M)	0.0753
Hydrogen Production (cm^3/min)	0.7167

Response	Fit	SE Fit	95% CI	95% PI
Hydrogen Production (cm^3/min)	0.5053	0.0495	(0.4021, 0.6086)	(0.2136, 0.7971)
StdOrder	29.98	7.21	(14.62, 45.33)	(8.86, 51.09)

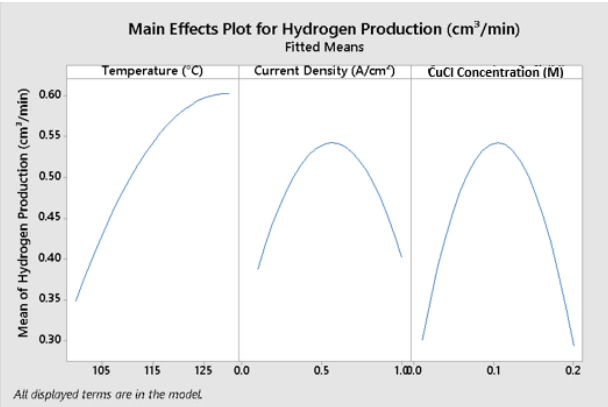

Fig. 6. Main effects plot for Hydrogen Production

software which explicitly tells us the best parameter settings to get the optimum hydrogen yield.

Each experiment has its own set of parameters to get the best yield. For this study, the chosen parameters were temperature (100 to 130°C), current density (0.1 to 1 A cm^{-2}) and CuCl concentration (0.01 to 0.2 M). The optimization of operating parameters was performed using Response Surface Methodology (RSM). The interaction plots in Figure 5 illustrate the effects of temperature, CuCl concentration, and current density on hydrogen yield. The highest hydrogen production was achieved at 116.67°C, 0.773 A/cm^2, and 0.075 M CuCl concentration, with a predicted yield of 0.7167 cm^3/min.

To validate this prediction, experimental results were obtained under optimized conditions. The actual hydrogen yield using the PBI/ZrP-based MEA was 0.7709 cm^3/min, which is 7.56% higher than the predicted value. In contrast, Nafion 117-based MEA produced 0.7085 cm^3/min, confirming the superior performance of the PBI/ZrP hybrid membrane in high-temperature CuCl electrolysis.

The hydrogen yield obtained using the PBI/ZrP hybrid membrane was compared to Nafion 117 and other PBI-based membranes (Table 3). The results revealed that the PBI/ZrP hybrid membrane achieved a hydrogen production rate of 0.7709 cm^3/min, which is 8.88% higher than Nafion (0.7085 cm^3/min). The improved yield is attributed to the membrane's superior thermal stability, reduced CuCl permeability, and higher proton conductivity.

Furthermore, the analysis of variance (ANOVA) results showed that temperature and current density significantly influenced hydrogen yield, with p -values of 0.000 and 0.026, respectively. These findings align with literature reports on high-temperature electrolysis systems, particularly regarding the significant influence of temperature and current density on hydrogen production efficiency [31].

4. Conclusion

The CuCl hydrogen electrolytic process parameters were optimized using RSM with CCD to determine the optimum value for each parameter that influences the hydrogen yield. The Pareto chart of the standardized effects of the hydrogen production compared the relative magnitude and the statistical significance of the main, square and interaction effects of the operating parameters, which squared concentration (CC), temperature (A) and squared current density (BB) that significantly influenced the hydrogen production. The analysis of variance (ANOVA) was statistically significant for the model, linear (temperature) and square (concentration*concentration and current density*current density). From the hydrogen yield data collected throughout the experiments, the Minitab 18 suggested that the optimized parameter settings for PBI/ZrP-based MEA were temperature at 116.7°C, current density at 0.773 A cm^{-2} and CuCl concentration at 0.075 M to obtain the optimum hydrogen yield of 0.7167 $cm^3\ min^{-1}$. The actual hydrogen yield for PBI/ZrP-based MEA from the optimized parameter settings was 0.7709 $cm^3\ min^{-1}$ with a discrepancy of 7.56% from the predicted value. Whereas the actual hydrogen yield for Nafion 117-based MEA at optimized parameter settings for PBI/ZrP was 0.7085 $cm^3\ min^{-1}$ which is 1.15% lower than the predicted hydrogen production and 8.88% lower than the actual hydrogen production for PBI/ZrP hybrid membrane. However, the increase of the effect of each parameter does not necessarily produce more hydrogen.

This study demonstrates the advantages of using the PBI/ZrP hybrid membrane for hightemperature CuCl electrolysis, with superior thermal stability, proton conductivity, and hydrogen yield compared to Nafion and conventional PBI membranes. The optimized process conditions further enhanced hydrogen production efficiency, reinforcing the feasibility of hybrid membranes for industrial-scale hydrogen production.

Therefore, optimizing the operating parameters is an important process to maximize the yield and minimize the associated cost for the CuCl hydrogen electrolytic process.

5. Acknowledgement

Financial support from the Universiti Putra Malaysia project number 945200 GP-IPM and Universiti Teknologi Malaysia project number 5L006 Research Officer Grant Scheme under the Malaysian Research Universities Network (MRUN) are acknowledged.

References

[1] I. K. Muritala, D. Guban, M. Roeb, and C. Sattler, (2020) *"High Temperature Production of Hydrogen: Assessment of Non-Renewable Resources Technologies and Emerging Trends"* **International Journal of Hydrogen Energy** ***45***(49): 26022–26035. DOI: 10.1016/j.ijhydene.2020.06.123.

[2] S. Kim, R. Schatz, S. Khurana, M. Fedkin, C. Wang, and S. Lvov, (2019) *"Advanced CuCl Electrolyzer for Hydrogen Production via the Cu–Cl Thermochemical Cycle"* **ECS Transactions** ***35***(32): 257. DOI: 10.1149/05001.0257ecst.

[3] D. M. Hall and S. N. Lvov, (2016) *"Modeling a CuCl (aq)/HCl (aq) Electrolyzer Using Thermodynamics and Electrochemical Kinetics"* **Electrochimica Acta** ***190***: 1167–1174. DOI: 10.1016/j.electacta.2015.12.123.

[4] O. A. Jianu, Z. Wang, M. A. Rosen, and G. F. Naterer, (2013) *"Shadow Imaging of Particle Dynamics and Dissolution Rates in Aqueous Solutions for Hydrogen Production"* **Experimental Thermal and Fluid Science** ***51***: 297–301. DOI: 10.1016/j.expthermflusci.2013.09.045.

[5] A. Farsi, C. Zamfirescu, I. Dincer, and G. F. Naterer, (2019) *"Thermodynamic Assessment of a Lab-Scale Experimental Copper-Chlorine Cycle for Sustainable Hydrogen Production"* **International Journal of Hydrogen Energy** ***44***(33): 17595–17610. DOI: 10.1016/j.ijhydene.2019.04.123.

[6] A. Farsi, " Kayhan, C. Zamfirescu, I. Dincer, and G. F. Naterer, (2019) *"Kinetic and Hydrodynamic Analyses of Chemically Reacting Gas-Particle Flow in Cupric Chloride Hydrolysis for the Cu–Cl Cycle"* **International Journal of Hydrogen Energy** ***44***(49): 26783–26793. DOI: 10.1016/j.ijhydene.2019.05.678.

[7] D. Bessarabov, H. Wang, H. Li, and N. Zhao, eds. *PEM Electrolysis for Hydrogen Production: Principles and Applications*. Boca Raton, FL: CRC Press, 2016. DOI: 10.1201/b20378.

[8] J. Ran, L. Wu, Y. He, Z. Yang, Y. Wang, C. Jiang, and T. Xu, (2017) *"Ion Exchange Membranes: New Developments and Applications"* **Journal of Membrane Science** ***522***: 267–291. DOI: 10.1016/j.memsci.2017.02.011.

[9] Q. Zhang, H. Liu, X. Li, R. Xu, J. Zhong, R. Chen, and X. Gu, (2016) *"Synthesis and Characterization of Polybenzimidazole/α-Zirconium Phosphate Composites as Proton Exchange Membrane"* **Polymer Engineering & Science** ***56***(6): 622–628. DOI: 10.1002/pen.24367.

[10] Z. Zhou, O. Zholobko, X. F. Wu, T. Aulich, J. Thakare, and J. Hurley, (2020) *"Polybenzimidazole-Based Polymer Electrolyte Membranes for High-Temperature Fuel Cells: Current Status and Prospects"* **Energies** ***14***(1): 135. DOI: 10.3390/en14010135.

[11] D. Aili, M. K. Hansen, C. Pan, Q. Li, E. Christensen, J. O. Jensen, and N. J. Bjerrum, (2011) *"Phosphoric Acid Doped Membranes Based on Nafion®, PBI and Their Blends–Membrane Preparation, Characterization and Steam Electrolysis Testing"* **International Journal of Hydrogen Energy** ***36***(12): 6985–6993. DOI: 10.1016/j.ijhydene.2011.03.058.

[12] Z. Mossayebi, T. Saririchi, S. Rowshanzamir, and M. J. Parnian, (2016) *"Investigation and Optimization of Physicochemical Properties of Sulfated Zirconia/Sulfonated Poly (Ether Ether Ketone) Nanocomposite Membranes for Medium Temperature Proton Exchange

Membrane Fuel Cells" **International Journal of Hydrogen Energy *41***(28): 12293–12306. DOI: 10.1016/j.ijhydene.2016.05.183.

[13] A. Villagra and P. Millet, (2019) *"An Analysis of PEM Water Electrolysis Cells Operating at Elevated Current Densities"* **International Journal of Hydrogen Energy *44***(20): 9708–9717. DOI: 10.1016/j.ijhydene.2019.02.120.

[14] F. Gashoul, M. J. Parnian, and S. Rowshanzamir, (2017) *"A New Study on Improving the Physicochemical and Electrochemical Properties of SPEEK Nanocomposite Membranes for Medium Temperature Proton Exchange Membrane Fuel Cells Using Different Loading of Zirconium Oxide Nanoparticles"* **International Journal of Hydrogen Energy *42***(1): 590–602. DOI: 10.1016/j.ijhydene.2016.09.124.

[15] A. Iulianelli and A. Basile, (2012) *"Sulfonated PEEK-Based Polymers in PEMFC and DMFC Applications: A Review"* **International Journal of Hydrogen Energy *37***(20): 15241–15255. DOI: 10.1016/j.ijhydene.2012.06.031.

[16] N. Shaari and S. K. Kamarudin, (2019) *"Recent Advances in Additive-Enhanced Polymer Electrolyte Membrane Properties in Fuel Cell Applications: An Overview"* **International Journal of Energy Research *43***(7): 2756–2794. DOI: 10.1002/er.4405.

[17] N. Abdo and E. B. Easton, (2016) *"Nafion/Polyaniline Composite Membranes for Hydrogen Production in the Cu–Cl Thermochemical Cycle"* **International Journal of Hydrogen Energy *41***(19): 7892–7903. DOI: 10.1016/j.ijhydene.2015.11.180.

[18] S. Giddey, S. P. S. Badwal, and H. Ju. "Polymer Electrolyte Membrane Technologies Integrated with Renewable Energy for Hydrogen Production". In: *Current Trends and Future Developments on (Bio-) Membranes*. Elsevier, 2019, 235–259. DOI: 10.1016/B978-0-12-814604-5.00010-6.

[19] N. Sathaiyan, V. Nandakumar, G. Sozhan, J. G. Packiaraj, E. T. Devakumar, D. Parvatalu, and B. N. Prabhu, (2015) *"Hydrogen Generation Through Cuprous Chloride-Hydrochloric Acid Electrolysis"* **International Journal of Energy Power Engineering *4***: 15–22.

[20] M. F. A. Kamaroddin, N. Sabli, P. M. Nia, T. A. T. Abdullah, L. C. Abdullah, S. Izhar, and A. Ahmad, (2020) *"Phosphoric Acid Doped Composite Proton Exchange Membrane for Hydrogen Production in Medium-Temperature Copper Chloride Electrolysis"* **International Journal of Hydrogen Energy *45***(42): 22209–22222. DOI: 10.1016/j.ijhydene.2020.06.050.

[21] J. Escorihuela, J. Olvera-Mancilla, L. Alexandrova, L. F. Del Castillo, and V. Compañ, (2020) *"Recent Progress in the Development of Composite Membranes Based on Polybenzimidazole for High Temperature Proton Exchange Membrane (PEM) Fuel Cell Applications"* **Polymers *12***(9): 1861. DOI: 10.3390/polym12091861.

[22] Y. Xiao, X. Shen, R. Sun, S. Wang, J. Xiang, L. Zhang, and N. Tang, (2022) *"Polybenzimidazole Membrane Crosslinked with Quaternized Polyaniline as High-Temperature Proton Exchange Membrane: Enhanced Proton Conductivity and Stability"* **Journal of Membrane Science *660***: 120795. DOI: 10.1016/j.memsci.2022.120795.

[23] H. Li, L. Stolberg, A. Vega, W. Zhang, S. Reinwald, D. Ryland, and S. Suppiah, (2020) *"Canadian Advances in the Copper–Chlorine Thermochemical Cycle for Clean Hydrogen Production: A Focus on Electrolysis"* **International Journal of Hydrogen Energy *45***(58): 33037–33046. DOI: 10.1016/j.ijhydene.2020.05.232.

[24] M. F. A. Kamaroddin, N. Sabli, T. A. T. Abdullah, S. I. Siajam, L. C. Abdullah, A. A. Jalil, and A. Ahmad, (2021) *"Membrane-Based Electrolysis for Hydrogen Production: A Review"* **Membranes *11***(11): 810. DOI: 10.3390/membranes11110810.

[25] N. I. Madondo, S. Rathilal, and B. F. Bakare, (2022) *"Utilization of Response Surface Methodology in Optimization and Modelling of a Microbial Electrolysis Cell for Wastewater Treatment Using Box–Behnken Design Method"* **Catalysts *12***(9): 1052. DOI: 10.3390/catal12091052.

[26] E. H. Gürkan, Y. Tibet, and S. Çoruh, (2021) *"Application of Full Factorial Design Method for Optimization of Heavy Metal Release from Lead Smelting Slag"* **Sustainability *13***(9): 4890. DOI: 10.3390/su13094890.

[27] M. F. A. Kamaroddin, N. Sabli, P. M. Nia, T. A. T. Abdullah, L. C. Abdullah, S. Izhar, and A. Ahmad, (2020) *"Phosphoric Acid Doped Composite Proton Exchange Membrane for Hydrogen Production in Medium-Temperature Copper Chloride Electrolysis"* **International Journal of Hydrogen Energy *45***(42): 22209–22222. DOI: 10.1016/j.ijhydene.2020.06.050.

[28] R. Soltani, I. Dincer, and M. A. Rosen, (2019) *"Kinetic and Electrochemical Analyses of a CuCl/HCl Electrolyzer"* **International Journal of Energy Research *43***(13): 6890–6906. DOI: 10.1002/er.4395.

[29] S. Toghyani, E. Afshari, E. Baniasadi, S. A. Atyabi, and G. F. Naterer, (2018) *"Thermal and Electrochemical Performance Assessment of a High-Temperature PEM Electrolyzer"* **Energy *152***: 237–246. DOI: 10.1016/j.energy.2018.03.140.

[30] S. Toghyani, E. Afshari, and E. Baniasadi, (2018) *"Metal Foams as Flow Distributors in Comparison with Serpentine and Parallel Flow Fields in Proton Exchange Membrane Electrolyzer Cells"* **Electrochimica Acta *290***: 506–519. DOI: 10.1016/j.electacta.2018.09.056.

[31] F. Scheepers, M. Stähler, A. Stähler, E. Rauls, M. Müller, M. Carmo, and W. Lehnert, (2021) *"Temperature Optimization for Improving Polymer Electrolyte Membrane-Water Electrolysis System Efficiency"* **Applied Energy *283***: 116270. DOI: 10.1016/j.apenergy.2020.116270.